Sustained adenosine release

Hajiali, Hadi; McLaren, Jane; Gonzalez-García, Cristina; Abdelrazig, Salah; Kim, Dong-Hyun; Dalby, Matthew J.; Salmerón-Sánchez, Manuel; Rose, Felicity R.A.J.

DOI:
10.1016/j.engreg.2024.04.002

Document Version
Publisher's PDF, also known as Version of record

Citation for published version (Harvard):
Hajiali, H, McLaren, J, Gonzalez-García, C, Abdelrazig, S, Kim, D-H, Dalby, MJ, Salmerón-Sánchez, M & Rose, FRAJ 2024, 'Sustained adenosine release: Revealing its impact on osteogenic signalling pathways of human mesenchymal stromal cells', *Engineered Regeneration*, vol. 5, no. 2, pp. 255-268. https://doi.org/10.1016/j.engreg.2024.04.002

Engineered Regeneration 5 (2024) 255–268

Contents lists available at ScienceDirect

Engineered Regeneration

journal homepage: http://www.keaipublishing.com/en/journals/engineered-regeneration/

Sustained adenosine release: Revealing its impact on osteogenic signalling pathways of human mesenchymal stromal cells

Hadi Hajiali[a,b,*], Jane McLaren[a], Cristina Gonzalez-García[c], Salah Abdelrazig[d,e], Dong-Hyun Kim[d], Matthew J. Dalby[c], Manuel Salmerón-Sánchez[c], Felicity R.A.J. Rose[a,*]

[a] School of Pharmacy, Nottingham Biodiscovery Institute, University of Nottingham, Nottingham, UK
[b] Healthcare Technologies Institute, School of Chemical Engineering, University of Birmingham, Birmingham, UK
[c] Centre for the Cellular Microenvironment, University of Glasgow, Glasgow, UK
[d] Centre for Analytical Bioscience, Advanced Materials & Healthcare Technologies Division, School of Pharmacy, University of Nottingham, Nottingham, UK
[e] Marine Microbiomics, Program in Biology, Division of Science and Mathematics, New York University Abu Dhabi (NYUAD), P.O. Box 129188, Abu Dhabi, United Arab Emirates

ARTICLE INFO

Keywords:
Adenosine release
Osteogenic signalling pathways
Human mesenchymal stromal cells
Bone regeneration

ABSTRACT

Non-healing fractures, a global health concern arising from trauma, osteoporosis, and tumours, can lead to severe disabilities. Adenosine, integral to cellular energy metabolism, gains prominence in bone regeneration via adenosine A_2B receptor activation. This study introduces a controlled-release system for localized adenosine delivery, fostering human mesenchymal stromal cell (hMSC) differentiation into functional bone cells. The study investigates how the ratio of lactic acid to glycolic acid in microparticles can influence adenosine release and explores the downstream effects on gene expression and metabolic profiles of osteogenic differentiation in hMSCs cultured in growth and osteoinductive media. Insights into adenosine-modulated signalling pathways during MSC differentiation, with osteogenic factors, provide a comprehensive understanding of the pathways involved. Analysing gene expression and metabolic profiles unravels adenosine's regulatory mechanisms in MSC differentiation. Sustained adenosine release from microparticles induces mineralization, synergizing with osteogenic media supplements, showcasing the potential of adenosine for treating critical bone defects and metabolic disorders. This study highlights the efficacy of a polymeric microparticle-based delivery system, offering novel strategies for bone repair. Unveiling adenosine's roles and associated signalling pathways advances our comprehension of molecular mechanisms steering bone regeneration, propelling innovative biomaterial, combined with metabolites, approaches for clinical use.

1. Introduction

Non-healing fractures arising from trauma, diseases such as osteoporosis, and tumours not only lead to bone loss but also impact millions of individuals, representing a major global cause of disability [1]. An example that illustrates the significant economic implications of such bone defects and disorders is the escalating expenses, reaching €37 billion per year for 3.5 million osteoporotic fractures in the European Union alone, with the costs anticipated to increase by 25 % in 2025 [2]. Clinically used biomaterials, such as metals, ceramics, polymers, and their composites, have limitations including low biocompatibility, inadequate bone formation, and a mismatch in mechanical properties with native bone. Delivery of factors, such as growth factors and small molecules, can support and augment new bone formation [3]. It is essential to control the spatio-temporal release kinetics of such factors to enhance their efficiency and reduce the side effects of their high dose, as seen with the use of BMP2 [3–6]. Therefore, many research projects have focussed on the development of controlled release delivery systems that accelerate and promote bone regrowth in defect sites [3].

Adenosine (Ad) is a molecule consisting of adenine and ribose and is one of four main constituents of nucleic acids (DNA and RNA). Its derivatives can serve as energy carriers including adenosine -monophosphate (AMP), -diphosphate (ADP), and -triphosphate (ATP). G protein-coupled receptors (GPCRs) are a large family of protein receptors that can bind to external stimuli which stimulates signalling cascades within the cell [7–9]. These receptors are able to sense different extracellular stimuli such as growth factors, metabolites, hormones, cytokines, neurotransmitters, and phospholipids to impact various cellular processes, including cell metabolism, proliferation, and differentiation [9,10]. Among the GPCRs, the adenosine A_{2B} receptors (A_{2B}ARs) have been shown to activate mesenchymal stromal cell (MSC) differentiation and enhance osteogenesis both *in vitro* and *in vivo*, suggesting that this receptor could be an innovative target for bone regeneration [11–15]. A_{2B}ARs are functionally activated by endogenous adenosine only in damaged and inflamed

* Corresponding authors.
E-mail addresses: hadi.hajiali@nottingham.ac.uk (H. Hajiali), felicity.rose@nottingham.ac.uk (F.R.A.J. Rose).

https://doi.org/10.1016/j.engreg.2024.04.002
Received 18 December 2023; Received in revised form 3 April 2024; Accepted 10 April 2024
Available online 12 April 2024

tissues in which adenosine is released in large doses following ATP degradation or they can be activated by an exogenous source through supplementing media with adenosine in an *in vitro* context. Gharibi et al. showed that activation and overexpression of the adenosine A_{2b} receptor ($A_{2b}R$) by supplementation of adenosine in osteoinductive media can induce the expression of osteoblast-related genes and activate the three stages of initiation, maturation, and mineralization in osteoblastogenesis of MSC [15]. Furthermore, some studies have been published and have illustrated that biomaterials consisting of calcium phosphate minerals can enhance the osteogenesis of human mesenchymal stromal cells (hMSCs) through phosphate–ATP–Adenosine-$A_{2b}R$ signalling [16,17]. In addition, Kang et al. reported that human induced pluripotent stem cells (hiPSCs) can be differentiated into functional osteoblasts by the supplementation of Adenosine in the culture media. The hiPSCs treated with adenosine expressed the markers of mature osteoblasts and produced a calcified bone matrix [18].

Furthermore, controlling the delivery of factors is essential for effective tissue regeneration. Incorporating factors into biomaterial carrier systems offers a means of achieving such control [5,6,19]. Various strategies, including non-covalent mechanisms (*e.g.*, physical entrapment, surface adsorption, and complexation) or covalent immobilization, can be employed to incorporate factors into delivery vehicles [19,20]. Polymeric microparticles have shown spatio-temporal control of factor release, allowing for precise regulation of duration and availability while minimizing side effects [6,19]. Furthermore, these microparticle-based scaffolds facilitate tissue formation and maintain desired local factor concentrations. Lactide and glycolide homo- and copolymers are particularly suitable as controlled delivery vehicles due to their FDA approval, *in vivo* biodegradability into natural products, and adjustable physicochemical properties [19,21].

In this study, we designed a controlled release delivery system for the localised release of adenosine within the defect site to induce hMSCs and osteoprogenitor differentiation and maturation into functional bone cells for bone regeneration. This study aimed to investigate the effect of the ratio of lactic acid to glycolic acid on the adjustment of adenosine release from microparticles designed for the local release of adenosine, and, at the same time, to analyse the impact of the released adenosine on the gene expression and the metabolic profiles of osteogenic differentiation of primary hMSCs cultured *in vitro* in growth and osteoinductive media for the first time. The incorporation of adenosine into PLGA microparticles marks a significant step forward in bone grafting and regenerative medicine. By embedding adenosine in biodegradable and biocompatible microparticles, this approach aims to create an advanced delivery system compatible with clinical practices for effectively treating bone defects and disorders.

Moreover, the precise effects of adenosine on the signalling pathways of MSCs in the presence of osteogenic factors remain poorly understood. In this study, we aimed to elucidate the role of adenosine in the presence or absence of osteogenic factors through comprehensive analysis of gene expression and metabolic profiles. By investigating the genes, metabolites, and molecular pathways involved in MSC differentiation, our findings provide novel insights into the impact of adenosine on MSC differentiation at the molecular level, thereby contributing to a better understanding of its regulatory mechanisms.

2. Methods and materials

2.1. Polymer microparticle fabrication

Polymer microparticles (MPs) were synthesized using a solid-in-oil-in-water (S/O/W) emulsion technique. In this method, adenosine (200 mg; Sigma-Aldrich, #A4036) was directly incorporated into the solid phase of poly(lactic-co-glycolic acid) (PLGA) (1000 mg) dissolved in dichloromethane (DCM). PLGA with various ratios of lactic acid to glycolic acid (75:25, 80:20, and 85:15) was used, namely PLGA 75:25 (Inherent Viscosity (IV): 0.56 dL/g; molecular weight (Mw): ~ 80 kDa), PLGA 80:20 (IV: 0.35 dL/g; Mw: ~ 39 kDa), and PLGA 85:15 (IV: 0.48 dL/g; Mw: 62 kDa), purchased from Ashland. The preparation of microparticles followed a previously published protocol [19]. Briefly, solid adenosine powder was added to PLGA solutions in DCM. These solutions were then added to a 200 mL 1 % (w/v) polyvinyl alcohol (PVA) solution and homogenized at 2000 rpm for two minutes (Fig. 1A). The resulting S/O/W emulsion was stirred at 600 rpm on a magnetic stirrer (Variomag 15-way) for a minimum of 4 h to allow for DCM evaporation. Microparticles underwent a thorough washing process involving three cycles in 50 mL tubes using deionized water. Each washing cycle consisted of centrifugation at 2000 xg for 5 min at room temperature. Subsequently, the formed particles were filtered using cell strainers with pore sizes of 40 μm and 100 μm, and only particles within the size range of 40 to 100 μm were collected for further investigation. Finally, the collected particles were subjected to lyophilization using an Edwards Modulyo freeze dryer (IMA Edwards, UK) until completely dried.

2.2. Preparation of 3D scaffolds based on microparticles

The produced microparticles were packed into a PTFE mould (100 mg for 24 well-plates, and 20 mg for 96 well-plate) and heated in an oven to 70 °C (higher than the glass transition temperature of PLGA) for 30 min. This induced microparticles to bond with neighbouring particles, forming a '2.5D' 300 μm-thick disc (6 or 14 mm diameter that could be placed in 96 and 24 well-plates, respectively, for further studies) (Fig. 1B). Discs, termed subsequently as 'scaffolds', were sterilized by UV irradiation for 30 min on both sides (15 min each side) and washed in PBS.

2.3. MP based-scaffold characterization

After scaffold preparation, the morphology and the efficiency of encapsulation of adenosine in the microparticles were evaluated. To examine the structure of the microparticles, the scaffolds were affixed to an adhesive stub and underwent gold sputter coating for a duration of four minutes at 30 mA (Balzers SCD 030 gold sputter coater, Balzers, Liechtenstein). Subsequently, the microparticles were visualized using a JSM 6060LV Scanning Electron Microscope (SEM) (JEOL, Welwyn Garden City, UK), operating at an accelerating voltage of 10 kV. The diameter of the microparticles was determined by processing the SEM images by ImageJ ($n = 100$).

Measurement of the encapsulation efficiency of adenosine within the microparticles was undertaken based on the photochemistry of adenosine. It has previously been demonstrated that adenosine absorbs light in the UV range [22]. Known concentrations (0–250 μg/ml) of adenosine were dissolved in PBS at room temperature and scanned UV absorbance with a wavelength from 230 nm to 310 nm (step size: 2 nm) using a plate reader (Tecan UK Ltd., Reading, UK) to find the wavelength of maximum absorption of adenosine which was 260 nm (Fig. S1). Adenosine was then dissolved in DMSO (as this would be the solvent for the PLGA microparticles) and diluted further to give a series of concentrations to prepare a standard curve (UV at 260 nm) (Fig. S2). Finally, 20 mg of PLGA/Ad scaffolds were dissolved to 2 ml DMSO, and the absorbance was measured at 260 nm. The standard curve was used to measure the actual amount of adenosine in each group of samples. The encapsulation efficiency was calculated through the measured amount of adenosine divided by the total adenosine added and expressed as a percentage.

2.4. Release study

MP-based scaffolds (14 mm diameter- 0.3 mm thickness fabricated with 100 mg of MP; triplicate samples from each batch) were submerged in 1 ml phosphate buffered saline (PBS, pH 7.4) and incubated at 37 °C for 50 days to closely mimic the conditions of our biological *in vitro* studies. At predefined time intervals (day 1, 2, 4, 7, 9, 11, 14, 16, 18, 21, 23,

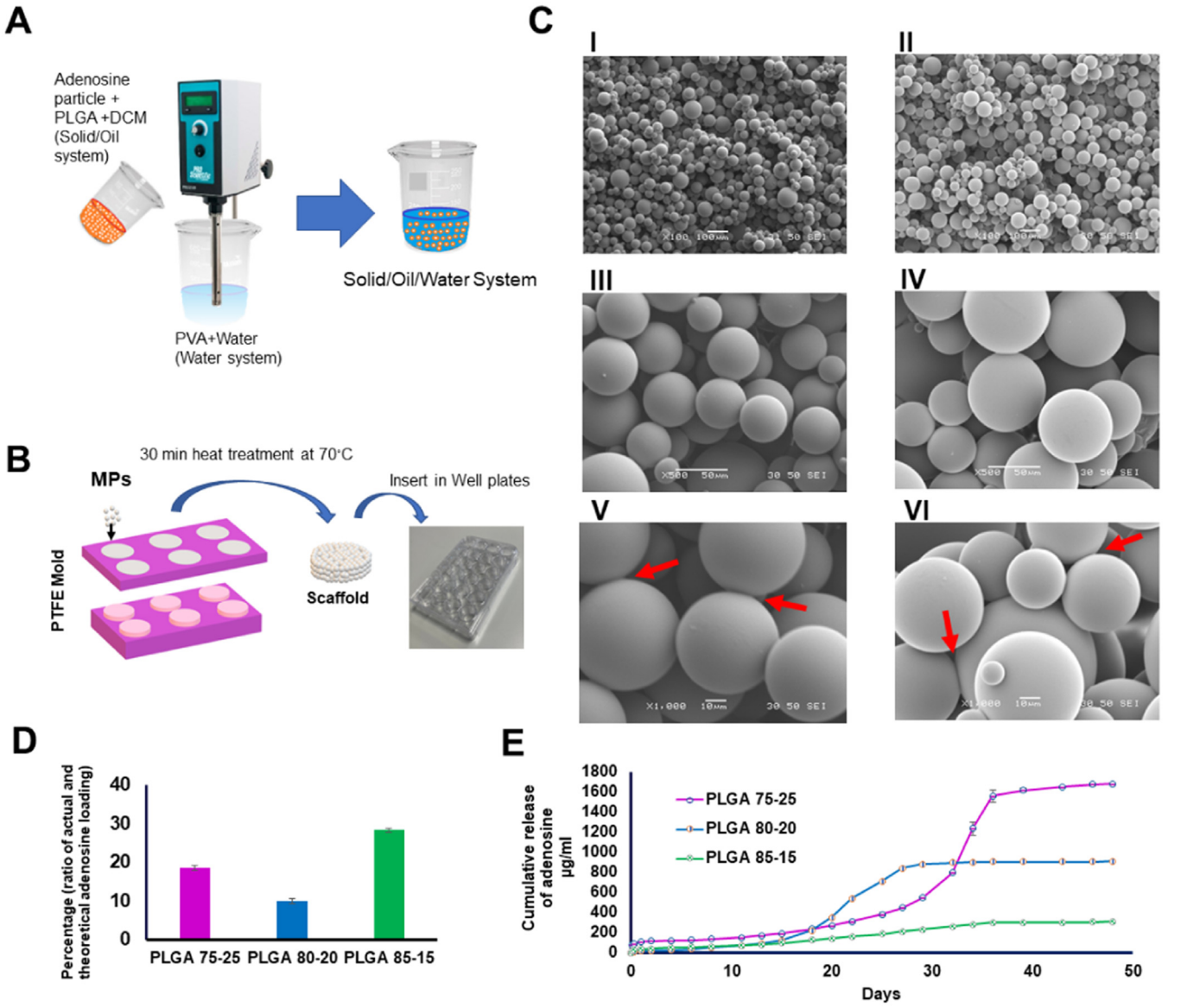

Fig. 1. Fabrication and characterization of PLGA microparticles with and without adenosine encapsulated in terms of morphology, loading efficiency, and release profile. (A) Schematic representation of microparticle fabrication using solid/oil/water emulsion (PLGA: poly(lactic-co-glycolic acid); PVA: polyvinyl alcohol; DCM: Dichloromethane). (B) Schematic showing the method used to fabricate scaffolds from microparticles for use in the experiments. (C) Representative SEM images of I,III,V: PLGA 80:20 microparticles; II,IV,VI: PLGA 80:20 with adensosine encapsulated microparticles with three magnifications of X100 (scale bar: 100 µm), X500 (scale bar: 50 µm), and X1000 (scale bar: 10 µm); red arrows indicate the fusion points between the microparticles. (D) the loading efficiency of adenosine in microparticles prepared using three ratios of PLGA (PLGA 75:25, PLGA 80:20, and PLGA 85:15); data is presented as means +/- SD; $n = 3$ (E): Cumulative release of adenosine from microparticles made by different polymers; data is presented as means +/- SD; $n = 3$.

25, 28, 30, 32, 35, 37, 39, 42, 44, and 46), PBS surrounding the scaffolds was aspirated and replaced with 1 ml of fresh PBS; all liquid above the particles was collected without removing scaffolds. This process was repeated every 2 to 3 days (coinciding with the media change in the aligned cell culture experiments). The collected supernatants were used to measure the amount of released adenosine by transferring 100 µL samples to a 96 well plate and reading the absorbance at 260 nm (Tecan UK Ltd., Reading, UK). Absorbance values were correlated to a standard curve of adenosine dissolved in PBS (0–250 µg/ml) (Fig. S3) to determine the release profile of adenosine.

2.5. hMSCs culture and osteogenic differentiation

Primary human bone marrow-derived mesenchymal stromal cells (hMSCs; #PT-2501, Batch No: 18TL262066 from Lonza) were obtained from Lonza (Germany) and cultured in the recommended maintenance media from Lonza including MSCBM Basal Media (#PT-3238; Lonza, Germany) and MSCGM Supplement Kit (#PT-4105; Lonza, Germany) within a humidified incubator with a controlled atmosphere of 5 % CO_2 in air at 37 ˚C. Based on certificate of analysis, these cells were tested for expression of surface markers correlated with hMSCs (positive for CD29, CD105, CD166, CD44, CD90, and CD 73, and negative for CD14, CD34, CD45, CD19, HLA-DR) [23] and for their ability to differentiate into osteogenic, adipogenic and chondrogenic lineages as confirmed in the certificate of analysis. The cells were used at passages 2 to 5 for all experiments. When used for experiments, cells were cultured on the scaffolds in the maintenance media to allow cell adhesion, and after 24 h of culture, the maintenance medium was replaced with a growth medium [GM: Dulbecco's modified Eagle's medium (DMEM), 10 % (v/v) foetal bovine serum, 4 mM L-glutamine, and penicillin/streptomycin (50 U/ml)] or osteogenic-inducing medium [OM: growth medium containing 10 mM b-glycerophosphate (BGP; Cal-

biochem, #35675), 50 mM ascorbic acid-2-phosphate (AAP; Sigma-Aldrich, #A8960), and 100 nM dexamethasone (DEX; Sigma-Aldrich, #D2915)]. The cells were seeded at a density of 5000 cells per square centimetre, resulting in a total of 10,000 cells per well in 24-well plates (TCP). For scaffolds with the size of 14 mm diameter, a seeding density of 20,000 cells per scaffold was used, which corresponds to a range of approximately 5000–10,000 cells/cm^2 based on the scaffold's surface area. The culture medium was refreshed every 2 to 3 days. In some experiments, GM or OM was supplemented with adenosine (30 μg/ml) (Sigma-Aldrich, #A4036) in every media exchange.

2.6. Immunostaining

The hMSCs were cultured on coverslips for 2 weeks as described above. The cells were seeded at a density of 10,000 cells per coverslip using the media described above. Samples were fixed in 4 wt% paraformaldehyde (PFA) in PBS for 20 min. Samples were then washed in PBS (3 × 5 min) and permeabilised with 0.1 % (v/v) Triton in PBS (PBST). Non-specific binding sites were blocked by incubation in 10 % (v/v) normal donkey serum (D9663; Sigma-Aldrich) and 1 % (v/v) bovine serum albumin (BSA) in PBS for 1 h. Cells were then incubated with anti-Osteocalcin antibody (AB10911; 1:250 in PBST; Merck Millipore), and Anti-CD105 antibody (ab69772; 1:250 in PBST; Abcam) overnight at 4 °C. Donkey anti-rabbit IgG-FITC, and Donkey anti-Mouse IgG- Alexa Fluor 546 Secondary antibodies, (1:500 in PBST; Invitrogen) were added for 2 h. The samples were washed again in PBST (3 × 5 min) and finally mounted with a pro-long gold mounting medium (Invitrogen) containing DAPI nuclear dye. Images were obtained using fluorescent microscopy (Leica Microsystems).

2.7. Alizarin red staining

2.7.1. Microscopy

Following a three-week culture period under various experimental conditions described above, Alizarin Red staining was performed to assess matrix mineralization. The spent media was aspirated, and the cells were rinsed thrice with calcium- and magnesium-free PBS (Sigma-Aldrich, D8537). Subsequently, the cells were fixed using 3.7 % (w/v) formaldehyde (Sigma-Aldrich, F8775) for 15 min at room temperature, followed by an additional three washes with distilled H2O. Next, 1 ml of Alizarin Red staining solution (40 mM, pH 4.1, sterile-filtered; Merck Millipore, TMS-008-C) was added to the cells, and they were incubated in darkness for 30 min at room temperature with gentle agitation. The staining solution was then removed, and cells were washed three times with dH_2O. Cells were immediately imaged at 0X (with a camera) and 10X magnifications (using a microscope).

2.7.2. Quantitation by absorbance

Following microscopy, to extract the Alizarin Red stain, water was removed, and 400 μL of 10 % (v/v) acetic acid in deionized water was added to the wells. Cells were incubated for 30 min in the dark with gentle agitation at room temperature. Cells were scraped from the culture surface, transferred to microcentrifuge tubes, and vortexed for 30 s. Samples were then heated to 85 °C for 10 min in an oven, and subsequently cooled on ice, before centrifugation at 20,000 xg for 15 min. Supernatants were then neutralized with 150 μL of 10% w/v ammonium hydroxide in deionized water before loading in triplicate in an opaque-walled 96-well plate, which included an Alizarin Red standard curve (0–4 mM). Absorbance was measured at 405 nm (Fig. S4), and the obtained data were further processed by normalizing them to the control conditions (without adenosine), and the results were represented as percentages relative to the control.

2.8. Gene expression studies

After seeding 20,000 hMSCs per optimized MP and MP/Ad scaffolds made of PLGA 80:20 in 24-well plates, the cells were cultured for a period of two weeks. The culture conditions included two distinct groups: growth media (GM) and osteogenic media (OM), as described earlier. Total RNA was isolated from hMSCs cultured under various experimental conditions for a duration of 2 weeks using the RNAqueous™-Micro Kit. Subsequently, the RNA from each sample was subjected to reverse transcription using the SuperScript™ IV First-Strand Synthesis System. The quality and quantity of RNA were assessed utilizing Agilent Technologies TapeStation. Quantitative real-time PCR was carried out using 96-well TaqMan® Gene Expression Array Cards according to the manufacturer's instructions. The PCR reactions were performed on a 7900HT Fast Real-Time PCR System with 384-Well Block Module (ThermoFisher Scientific). For normalization, endogenous control was employed, with GAPDH selected as the internal housekeeping gene. Genes exhibiting consistent replicates and a Ct value not exceeding 37 were considered for analysis. Three independent experiments were run (n = 3), and data were analysed using the Reactome software (source: https://reactome.org/). p-values were adjusted using the False Discovery Rate (FDR). Pathways found differentially expressed at an adjusted p-value <= 0.05 were considered to be significantly altered in their expression.

2.9. Untargeted metabolomics using LC-MS

All chemicals and reagents used for LC-MS analysis and metabolite identification are detailed in the Supporting Information.

2.9.1. Sample preparation

After 2 weeks of culturing hMSCs on different scaffold types, the spent media was collected and centrifuged at 10,000 xg for 5 min. Aliquots (250 μl) were transferred into a new tube for protein precipitation and metabolite extraction by addition of 750 μl cold methanol (stored at – 20 °C), mixing and incubating at – 20 °C for 20 min. Samples were then centrifuged at 17,000 × g at 4 °C for 10 min, transferred to pre-cooled tubes, and stored at −80 °C. Fresh culture medium samples and a methanol blank were processed in parallel as no-cell blanks. Samples were prepared with six replicates, where each group of the experiment consisted of cells cultured in six scaffolds prepared from MPs. Samples (methanolic extracts) were transferred to HPLC vials. Based on our previous study [24], 20 μl from each sample were collected and pooled together, vortexed for 30 s, transferred (>100 μl) into an HPLC vial with 200 μl glass insert, and used as a pooled QC to assess the instrument performance.

2.9.2. LC-MS analysis

Chromatography was conducted utilizing a Dionex U3000 UHPLC system (Thermo Fisher Scientific, Hemel Hempstead, UK) equipped with a ZIC-pHILIC column (4.6 × 150 mm, 5 μm particle size, Merck Sequant, Watford, UK). The column temperature was maintained at 45 °C, and a flow rate of 300 μL/min was employed. The mobile phases consisted of (A) 20 mM ammonium carbonate and (B) acetonitrile. The gradient commenced with 20 % (A) and was elevated to 95 % (A) over 8 min, followed by a return to initial conditions in 2 min. The column was then allowed to re-equilibrate at 400 μL/min for 4 min before reverting to 300 μl/min in 1 min, totalling 15 min. A sample injection volume of 5 μl was utilized, and samples were maintained at 4 °C during analysis. High-resolution Quadrupole-Orbitrap mass spectrometry (QExactive Plus, Thermo Fisher Scientific, Hemel Hempstead, UK) was employed in simultaneous ESI+ and ESI- modes for comprehensive LC-MS profiling and data-dependent MS/MS (ddMS/MS). The operational settings comprised a spray voltage set at 4.5 kV for ESI+ mode and 3.5 kV for ESI- mode. Additionally, the capillary voltage was adjusted to 20 V (ESI+) and −15 V (ESI-), while the flow rates of sheath, auxiliary, and sweep gases were set at 40, 5, and 1 (arbitrary unit), respectively, for both modes. The capillary and heater temperatures were maintained at 275 and 150 °C, respectively. Data were collected in full scan mode with a resolution of 70,000 within the m/z range of 70–1050. Moreover, the top

5 ddMS/MS scans were conducted at a resolution of 17,500, employing a stepped normalized collision energy (NEC) of 10, 20, and 40.

2.9.3. Untargeted metabolic profiling and metabolite identification using LC-MS

The extracted samples underwent randomization and analysis in a solitary analytical run following the inclusion of blanks ($n = 3$) using LC-MS in simultaneous positive and negative ion modes. Before analysing the samples, the column was equilibrated by conducting six injections of pooled QC samples at the onset of the sample run. To monitor the performance of the analytical system, pooled QC injections were interspersed throughout the run. For metabolite identification, 268 authentic standards were co-analysed with the samples under the same instrument conditions. In addition, QC sample ($n = 3$) was analysed using Top5 ddMS/MS to generate MS/MS accurate mass spectra for identification (see Supporting Information for full details of metabolite identification).

2.9.4. Data and pathway analysis

The acquired LC-MS datasets were analysed using principal component analysis (PCA) and orthogonal partial least-squares discriminant analysis (OPLS-DA) (Simca $P + 13$, Sartorius, Sweden) (full details of multivariate analysis are available in Supporting Information).

The peak areas of the altered metabolites in the samples were processed for metabolite enrichment, pathway, and network analysis using MetaboAnalyst 5.0 [25].

2.10. Statistical analysis

All data is presented as means +/- Standard Deviation (SD). Throughout the conducted experiments, the notation "n" is used to represent the number of technical replicates derived from a single batch of microparticles or a specific cell donor. In cases where a different number of replicates is employed, the exact value is explicitly stated and clarified in the respective experimental descriptions. Statistical significance at 95 % confidence level was determined using one-way/two-way ANOVA with post-hoc Tukey tests, and statistically significant differences were marked with * for $p < 0.05$, ** for $p < 0.01$, *** for $p < 0.001$, and **** for $p < 0.0001$ in the figures. Sample replicates using multiple scaffolds were used in all experiments, as detailed in the figure legends.

3. Results

3.1. Characterization of adenosine-loaded microparticles for controlled release (morphology and loading efficiency)

Microparticles (MP) encapsulating adenosine were fabricated using the S/O/W double emulsion technique. To modulate the release profile, three different formulations were prepared by varying the lactide:glycolide (LA:GA) ratio. The formulations consisted of PLGA 75:25 (Inherent Viscosity [IV]: 0.56 dl/g; molecular weight [Mw]: ~80 kDa), PLGA 80:20 (IV: 0.35 dl/g; Mw: ~39 kDa), and PLGA 85:15 (IV: 0.48 dl/g; Mw: 62 kDa). The morphology, loading efficiency, and *in vitro* release profile of adenosine were characterized for each formulation. The SEM images of MP morphology are shown in Fig. 1C (I, II, III, IV, V, and VI; MP fabricated from each of the three formulations were spherical, and their surfaces were smooth and non-porous. Higher magnification SEM images provide detailed visual evidence of the scaffold structure, specifically highlighting the successful fusion between MPs elucidating the interconnected network formed by the microparticles. Incorporation of adenosine did not affect the morphology of the microparticles significantly, as shown in the representative example of blank PLGA 80:20 and encapsulated adenosine in the PLGA 80:20 (Fig. 1C-I, 1C-III). The mean diameter of the microparticles was determined by analysing SEM images using ImageJ software. In the absence of adenosine (Fig. 1C-I), the mean diameter was found to be 90.8 μm (SD ± 24.7), while in the presence of adenosine (Fig. 1C-II), the mean diameter was measured to be 94.0 μm (SD ± 27.6). However, statistical analysis indicated that the observed difference in mean diameter between the two groups was not statistically significant.

The adenosine encapsulation efficiency ranged from 10 % to 30 % was obtained across all formulations (Fig. 1D). The experimental results revealed that the encapsulation efficiency of adenosine was determined to be 9.9 % ± 0.7 in the PLGA 80:20 microparticles (MP), 18.5 % ± 0.7 in the PLGA 75:25 MP, and 28.2 % ± 0.4 in the PLGA 85:15 MP. This finding indicates that the encapsulation of approximately 0.91 mg of adenosine within 100 mg of the PLGA 80:20 scaffold, 1.68 mg of adenosine within 100 mg of the PLGA 75:25 scaffold, and 2.56 mg of adenosine within 100 mg of the PLGA 85:15 scaffold was achieved. Employing the solid in oil in water (S/O/W) emulsion technique markedly enhanced adenosine encapsulation efficiency within the MPs as compared with a water in oil in water (W/O/W) system. Preliminary studies utilizing the water in oil in water (W/O/W) system, wherein adenosine was solubilized in water before integration into the system, yielded MPs with substantially low encapsulation efficiencies (Fig. S5). This data illustrates the shortcomings of the W/O/W double emulsion method for polymer encapsulation for controlled release. Following MP preparation using the W/O/W system, we recorded a negligible encapsulation efficiency, indicating a rapid burst release of adenosine during the washing phase, which resulted in an almost complete depletion of adenosine from the microparticles. In contrast, the S/O/W emulsion methodology efficiently entrapped adenosine molecules within the polymer matrix of the MPs.

3.2. Release profiles of adenosine from PLGA-Based MP scaffolds support selection of PLGA 80:20 composition

The cumulative release of adenosine from the MP/Ad scaffolds over one month is presented in Fig. 1E. The release profiles of adenosine differ among the three microparticle formulations: PLGA 80:20, PLGA 75:25, and PLGA 85:15. The PLGA 80:20 microparticles exhibit a relatively faster release rate, with adenosine release completing within 4 weeks. The cumulative amount of adenosine released steadily increases until reaching a plateau after 30 days. In contrast, the PLGA 75:25 and PLGA 85:15 microparticles demonstrate a slower release profile, sustaining adenosine release over a longer period. The PLGA 75:25 microparticles exhibit the highest amount of adenosine released after 6 weeks.

Focusing on the initial 2-week release period, the PLGA 80:20 microparticles display sustained release, indicating controlled release kinetics. This sustained release results in a consistent amount of adenosine being released over time. Analysis of the average daily release of adenosine from the various microparticle formulations reveals a sustained release ranging between 7.5 μg/ml and 30 μg/ml every 2 days during the first 2 weeks for the PLGA 80:20 microparticles with a total of 900 μg/ml release over 30 days. These findings support the selection of the PLGA 80:20 microparticle scaffold for further biological studies. To ensure consistency, we conducted experiments comparing the release profiles of freshly prepared batches with a stored batch in the fridge. No significant differences were observed (Fig. S6). These results further validate the reproducibility of the release profiles. Therefore, the cumulative release data demonstrates the distinct release profiles of adenosine from the different microparticle formulations, highlighting the potential for tailored release kinetics based on the choice of PLGA composition. The PLGA 80:20 microparticles, with their faster release rate and sustained release profile, show promise for controlled adenosine delivery applications and were investigated further in this study.

3.3. hMSCs osteodifferentiation in media supplemented with adenosine

Primary hMSCs were cultured in growth medium (GM), osteoinductive medium (OM), or OM supplemented with adenosine, and their

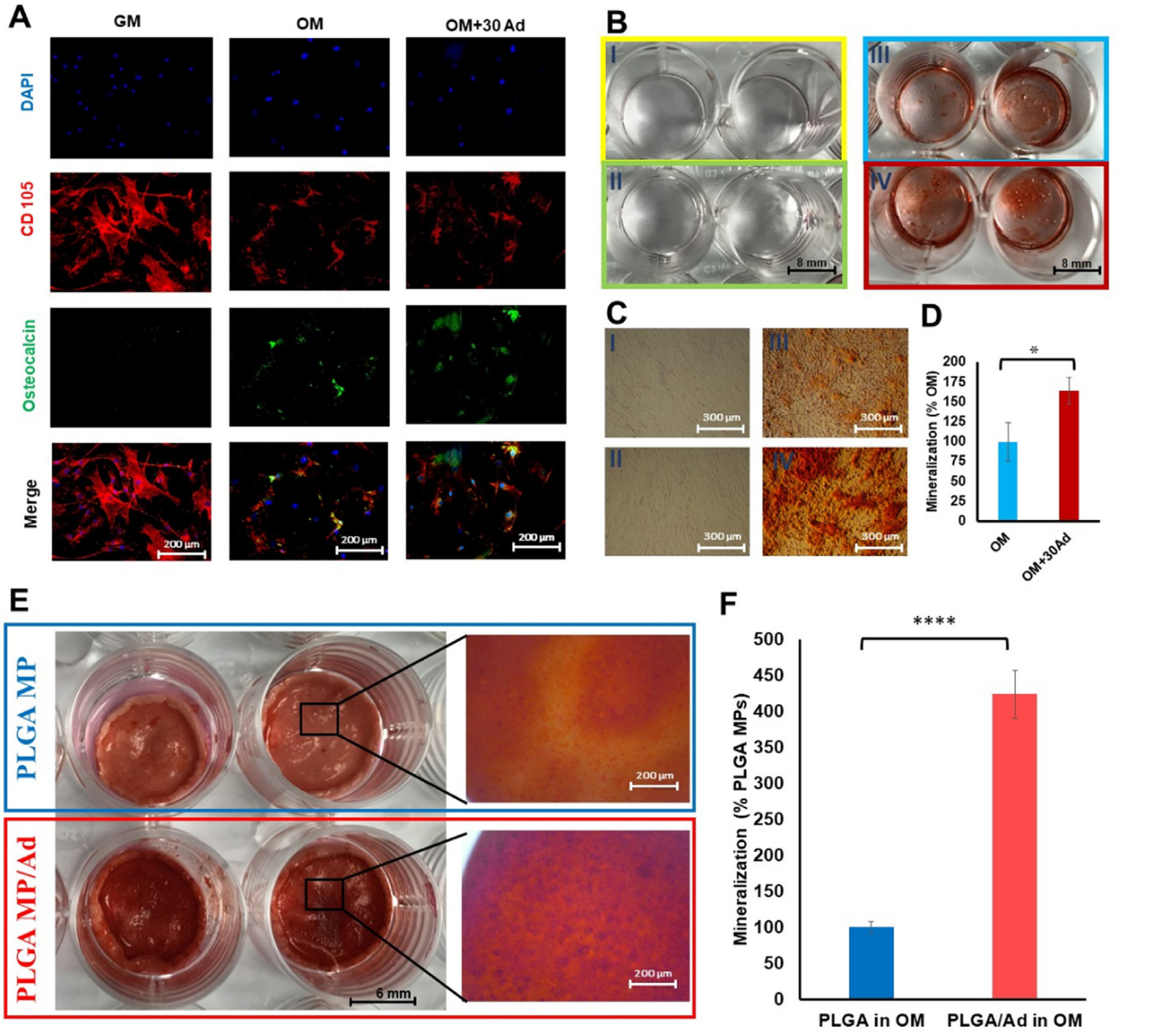

Fig. 2. Adenosine (Ad) synergizes with osteoinductive media (OM) enhancing the osteogenic differentiation and mineralization of hMSCs. (A) Immunostaining and fluorescence microscopy imaging of primary hMSCs cultured in different media including growth media (GM), OM, and 30 µg/ml adenosine supplemented OM for 14 days. Cell nuclei (DAPI) are shown in blue, CD105 in red, and osteocalcin (OCN) in green. (B,C,D) Mineralization of hMSCs following treatment with adenosine (30 µg/ml) in GM: growth media, and OM: osteoinductive media after 21 days. (B) Representative microscopy imaging of I: GM; II: GM + 30 µg/ml Ad; III: OM; IV: OM + 30 µg/ml Ad. (C) Representative light photograph I: GM; II: GM + 30 µg/ml Ad; III: OM; IV: OM + 30 µg/ml Ad. (D) Quantified mineralization results following elution of Alizarin Red and subsequent spectrophotometric measurement at 405 nm; data were normalized to the control conditions (without adenosine), and the results were represented as percentages relative to the control. (data is presented as means +/- SD, $n = 3$, * $p < 0.05$). (E, F) Mineralization of hMSCs cultured on PLGA microparticles (PLGA MP) alone and PLGA 80:20 MP/Ad in OM after 21 days. (E) Representative light photography and microscopy imaging of PLGA MP and PLGA MP/Ad. (F) Quantified mineralization results following elution of Alizarin Red S and subsequent spectrophotometric measurement at 405 nm; data were normalized to the control conditions (without adenosine), and the results were represented as percentages relative to the control. (data is presented as means +/- SD, $n = 3$, **** $p < 0.0001$).

osteogenic differentiation was determined after 14 days. The differentiation of hMSCs into osteoblasts was evaluated by immunofluorescence staining for osteocalcin (an osteoblast-specific marker) in the OM supplemented with adenosine compared to OM without adenosine (Fig. 2A). The intensity of CD105, a marker attributed by The International Society for Cellular Therapy as a marker of hMSC [23], was less intense when cells were cultured in OM and OM/Adenosine (30 µg/ml supplemented in the media) suggesting that these cells were undergoing differentiation. To further confirm osteogenic differentiation of the hMSCs, we evaluated the calcification of cell cultures by staining for Alizarin Red S. The hMSCs were cultured in both OM and adenosine-supplemented OM (30 µg/ml) and stained for Alizarin Red after 21 days of culture (Figs. 2B-III, 2B-IV, 2C-III, 2C-IV, and 2D). This extended culture duration of 21 days was chosen over the conventional 14-day period to allow for the development of calcification within the cells, as calcification processes typically require a longer incubation period to manifest fully. Similar to osteocalcin, the intensity for Alizarin Red staining was significantly enhanced by 64.5 % for the OM supplemented with Adeno-

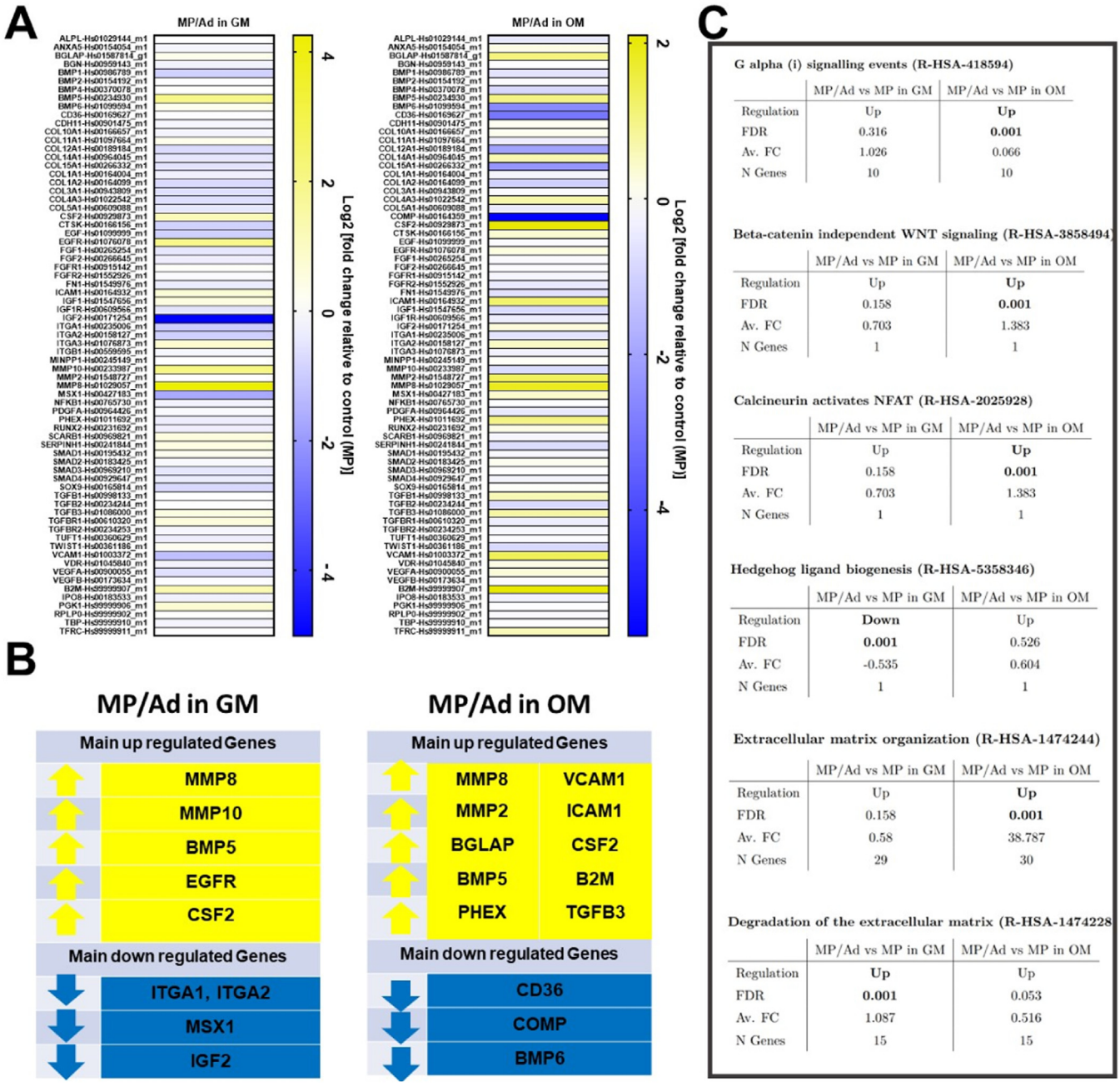

C

G alpha (i) signalling events (R-HSA-418594)

	MP/Ad vs MP in GM	MP/Ad vs MP in OM
Regulation	Up	**Up**
FDR	0.316	**0.001**
Av. FC	1.026	0.066
N Genes	10	10

Beta-catenin independent WNT signaling (R-HSA-3858494)

	MP/Ad vs MP in GM	MP/Ad vs MP in OM
Regulation	Up	**Up**
FDR	0.158	**0.001**
Av. FC	0.703	1.383
N Genes	1	1

Calcineurin activates NFAT (R-HSA-2025928)

	MP/Ad vs MP in GM	MP/Ad vs MP in OM
Regulation	Up	**Up**
FDR	0.158	**0.001**
Av. FC	0.703	1.383
N Genes	1	1

Hedgehog ligand biogenesis (R-HSA-5358346)

	MP/Ad vs MP in GM	MP/Ad vs MP in OM
Regulation	**Down**	Up
FDR	**0.001**	0.526
Av. FC	-0.535	0.604
N Genes	1	1

Extracellular matrix organization (R-HSA-1474244)

	MP/Ad vs MP in GM	MP/Ad vs MP in OM
Regulation	Up	**Up**
FDR	0.158	**0.001**
Av. FC	0.58	38.787
N Genes	29	30

Degradation of the extracellular matrix (R-HSA-1474228

	MP/Ad vs MP in GM	MP/Ad vs MP in OM
Regulation	**Up**	Up
FDR	**0.001**	0.053
Av. FC	1.087	0.516
N Genes	15	15

Fig. 3. Genetic profiles of hMSCs when cultured on microparticles (MP) and microparticles/adenosine (MP/Ad) in growth media (GM) compared with osteoinductive media (OM) for 14 days. (A) Gene profiling showed up-and down-regulated genes in hMSCs cultured on MP/Ad in GM and OM relative to control (MP). Relative gene expression is plotted as log2 (fold change) relative to control after normalization against the housekeeping gene (GAPDH) Yellow indicates upregulated and blue indicates downregulated genes ($n = 3$). (B) List of the main genes up regulated and down regulated genes in hMSCs cultured on MP/Ad in GM and OM relative to control (MP). (C) Significantly up- and down- regulated signalling pathways affected by culturing hMSCs on MP/Ad in GM and OM generated using the Reactome software.

sine compared to OM. On the contrary, no calcification was observed when the hMSCs were cultured in the growth medium (Figs. 2B-I, 2B-II, 2C-I and 2C-II).

3.4. hMSCs cultured on the PLGA MP-based scaffolds with sustained release of adenosine

3.4.1. Mineralization

Primary human mesenchymal stromal cells were seeded onto PLGA 80:20 MP and MP/Ad scaffolds and cultured in osteogenic induction media for 21 days. During this period, adenosine was released from the PLGA 80:20 MP/Ad scaffolds. Alizarin Red S staining was conducted to evaluate the mineralization and hence differentiation of hMSCs to the osteoblast lineage. Alizarin Red staining and quantification illustrated a significant increase in mineralization when hMSCs were cultured on PLGA 80:20 MP scaffolds releasing adenosine (total loading amount: 0.91 mg of adenosine within 100 mg MPs in scaffolds) after 3 weeks of induction (Fig. 2E and 2F) when compared to MP discs not containing adenosine. Microscopy imaging also demonstrated enhanced calcification in the PLGA 80:20 MP/Ad samples (Fig. 2E). Quantification of Alizarin Red S staining indicated higher levels of mineralisation when cells were cultured on MP disks releasing adeno-

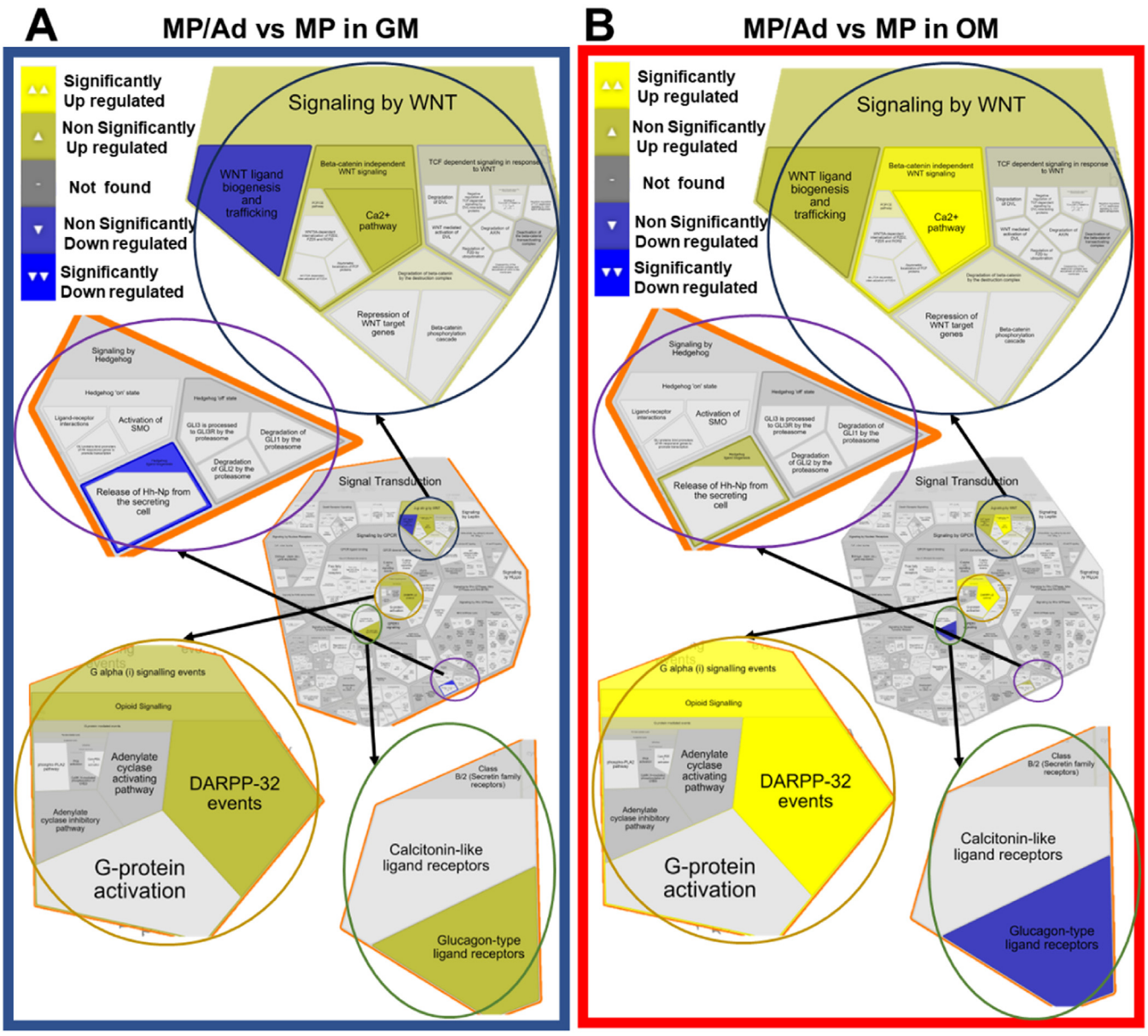

Fig. 4. An overview of the significantly up- and down- regulated transduction signalling pathways were affected by culturing primary hMSCs on MP/Ad in (A) GM and (B) OM generated using the Reactome software.

sine as compared with cultures on MP discs composed of PLGA alone (Fig. 2F).

3.4.2. Gene expression

The genetic profile of hMSCs cultured on PLGA 80:20 MP/Ad scaffolds and MP with no adenosine in both osteoinductive (OM) and growth media (GM) were compared following 14 days in culture. Analysis of data from cells cultured on PLGA 80:20 MP/Ad samples resulted in significantly different genetic responses compared to those cells cultured on MP with no adenosine samples (Fig. 3). When cells were cultured in GM (on the MP scaffolds), genes for MMP8 (4.4 fold), MMP10 (20.6 fold), BMP5 (4.14 fold), EGFR1 (11.8 fold), and CSF2 (2.3 fold) were differentially upregulated in cells cultured on PLGA 80:20 MP/Ad relative to those cultured on blank MP (no adenosine).

The pathway analysis from cells cultured on PLGA 80:20 MP/Ad scaffolds in GM using the Reactome software showed that the gene pathways upregulated including those encoding for proteins involved in the degradation of the extracellular matrix (matrix-metalloproteinases; MMP), extracellular matrix organization, G alpha (i) signalling, and signalling by WNT. In contrast, genes involved in the hedgehog ligand biogenesis pathway were significantly downregulated in cells cultured on PLGA 80:20 MP/Ad in GM.

In addition, the data obtained from cells cultured on PLGA 80:20 MP/Ad scaffolds in OM displayed an upregulation of BGLAP (2.5 fold), MMP2 (7.2 fold), MMP8 (4.4 fold), BMP5 (2.2 fold), and PHEX (2.0 fold) and downregulation of CD36, COMP, and BMP6 genes. Furthermore, the pathway analysis from OM cultured samples using the Reactome software demonstrated that the pathways including signalling by GPCR, G alpha (i) signalling, Beta-catenin independent WNT signalling, and extracellular matrix organization were significantly upregulated, and the glucagon type ligand-receptor pathway was downregulated when cells were cultured on PLGA 80:20 MP/Ad (Fig. 4).

3.4.3. Untargeted metabolomics and pathway analysis

Alterations in the genomic profile are often accompanied by changes in metabolic pathways [26], making metabolomics an appropriate method to assess cellular molecular signalling. Extracellular metabolite levels can be linked to intracellular metabolism [24]. The metabolic

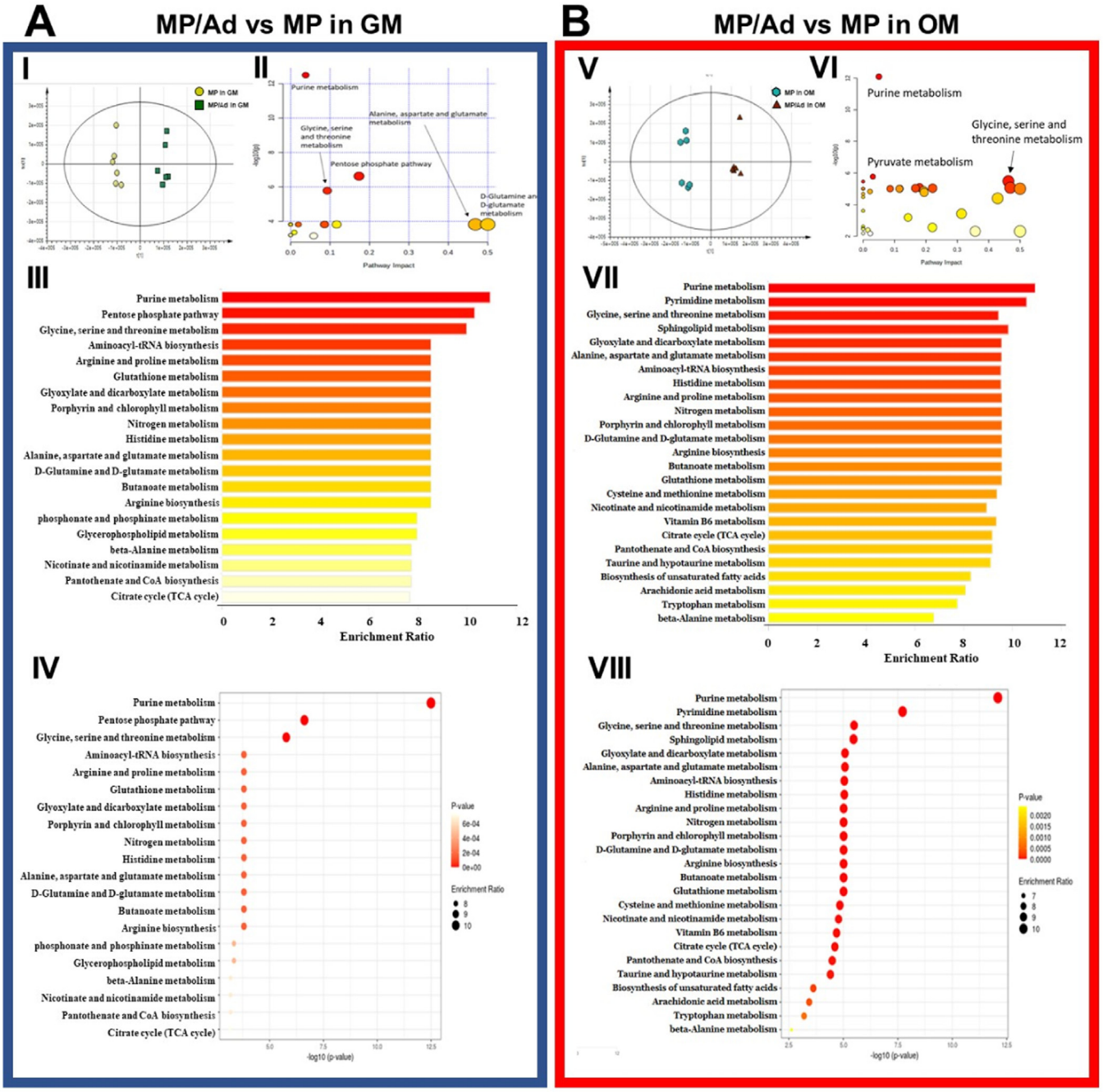

Fig. 5. Significant changes in the metabolic profiles of hMSCs cultured on microparticles (MP) compared to microparticles containing adenosine (MP/Ad) in (A) growth media (GM) and (B) osteoinductive media (OM). (A-I) and (B-V): OPLS-DA score plots of the metabolic profiling of the spent media of MP/Ad *versus* MP in GM (R^2X = 0.358, R^2Y = 0.984 and Q^2 = 0.709) and OM (R^2X = 0.494, R^2Y = 0.985 and Q^2 = 0.886), respectively. (A-II) and (B-VI): Metabolite pathway analysis of the altered metabolites in MP/Ad compared to MP in GM and OM, respectively. The colour and size of each circle represent p values and pathway impact values, respectively (Darker colours signify more influential changes in the pathway, and size represents the centrality of involved metabolites; 'centrality' refers to the relative importance or prominence of these metabolites within the pathway). (A-III, IV) and (B-VII, VIII): Enrichment analyses of the top significantly altered metabolites in MP/Ad compared to MP in GM and OM, respectively. R^2X/R^2Y: fitness of the model and Q^2: predictive ability of the OPLS-DA based on Cross-Validation.

profiles of hMSCs cultured on PLGA 80:20 MP/Ad scaffolds were compared to those of hMSCs cultured on PLGA 80:20 MP scaffolds without adenosine. This comparison was conducted in both osteoinductive (OM) and growth media (GM) following a 14-day culture period. Samples of culture media were analysed using LC-MS on day 14 post-culture to investigate adaptive metabolic changes occurring in hMSCs cultured on microparticles. PCA was used to check for the performance of the LC-MS (data not shown) and OPLS-DA to identify significant differences in the metabolic profiles between the different classes of the samples. OPLS-DA scores plot showed adequate clustering of biological replicates in each class of samples and highlighted distinct differences in the metabolic profiles of hMSCs cultured on different microparticles and media (Fig. 5A-I, and 5B-V); different classes of samples showed distinct clustering from each other (Fig. S7). This result indicates that the release of adenosine from microparticles either in growth media or osteoinductive media resulted in cells transitioning to a metabolic state different

from that of cells cultured on blank microparticles (no adenosine; Fig. 5A and 5B). Certain metabolites were found significantly altered in the spent media from cells cultured (in GM and OM) on PLGA 80:20 MP/Ad samples relative to blank MP (no adenosine); the full list of the identified metabolites is available in Table S1. Enrichment and pathway analysis of the altered metabolites in cells cultured on MP/Ad compared to MP in GM (Table S2) showed significant changes in purine metabolism, pentose phosphate pathway, (glycine, serine and threonine) metabolism, (arginine and proline) metabolism, glutathione metabolism, (alanine, aspartate and glutamate) metabolism, (D-glutamine and D-glutamate) metabolism, arginine biosynthesis, and the citrate cycle (TCA cycle).

In addition, significantly altered metabolic pathways of hMSCs cultured on PLGA 80:20 MP/Ad in osteoinductive media (OM) were found compared to hMSCs cultured on blank MP (no adenosine) including purine metabolism, pyruvate metabolism, (glycine, serine, and threonine) metabolism, (glyoxylate and dicarboxylate) metabolism, (alanine, aspartate, and glutamate) metabolism, aminoacyl-tRNA biosynthesis, histidine metabolism, (arginine and proline) metabolism, arginine biosynthesis, (D-glutamine and D-glutamate) metabolism, glutathione metabolism, the citrate cycle (TCA cycle), and the pentose phosphate pathway.

4. Discussion

In this study, we have developed a controlled release delivery system aimed at facilitating the localized release of adenosine. This release is intended to trigger the differentiation and maturation of hMSCs into functional bone cells, ultimately promoting bone regeneration. Finally, we aimed to elucidate the role of adenosine in the presence or absence of osteogenic factors through a comprehensive analysis of gene expression and metabolomics. We hypothesized that the ratio of lactic acid to glycolic acid in the microparticles will significantly influence the modulation of adenosine release kinetics. In addition, we postulated that the released adenosine will have a discernible impact on the gene expression and the metabolic profiles of primary hMSCs undergoing osteogenic differentiation.

Microparticles (MP) with encapsulated adenosine (MP/Ad) were fabricated using S/O/W emulsion methodologies using three different formulations by varying the lactide: glycolide ratio (75:25, 80:20, and 85:15) with an average microparticle diameter of approx. 100 μm. The adenosine encapsulation efficiency ranged from 10 % to 30 % with the lowest encapsulation efficiency observed in microparticles composed of PLGA 80:20 and highest in PLGA 85:15 with molecular weight most likely to be the influencing factor on encapsulation efficiency [27]. The smaller molecular chains of PLGA 80:20 (39 kDa) reduced the chance of adenosine entrapment within the microparticles and resulted in a lower loading efficiency. This could be attributed to the lower viscosity of the polymeric solution, as a result of the low molecular weight of the polymer, preventing the transfer of adenosine from the solid/oil phase to the aqueous phase. Alternatively, the impact of molecular weight on encapsulation efficiency could be attributed to the attraction forces between adenosine and the polymer chains which could also cause the entrapment of lower amounts of adenosine. Ravi et al [27] also showed that the encapsulation efficiency was highly influenced by the molecular weight and hydrophilicity of PLGA polymers. They showed that the protein encapsulation efficiency was higher when using higher molecular weight polymers In our study, a higher encapsulation efficiency was observed for the PLGA 85:15 polymer (62 kDa) compared to PLGA75:25 (80 kDa). This might be due to the higher crystallinity and lower hydrophilicity of PLGA 85:15 rather than PLGA 75:25. The properties of PLGA can be modulated by changing the ratio of the two monomers where each monomer shows different properties; for example, LA degrades more slowly and is hydrophobic, while GA is relatively less hydrophobicity and degrades more quickly [28]. In fact, increasing the content of the LA monomer in PLGA polymer increases the hydrophobicity of the polymer and reduces the amorphous nature of the polymer [28,29]. The higher crystallinity of PLGA 85:15 compared to PLGA 75:25 might improve the adenosine entrapment in the microparticles and result in higher loading efficiencies. Elevated crystallinity may restrict the mobility of adenosine within the microparticles, potentially leading to altered release rates. Essentially, while a higher crystalline structure might improve initial loading, it could simultaneously decelerate adenosine release by reducing the amorphous regions within the polymer matrix.

The release data showed a faster and more sustained release of adenosine from MP fabricated from PLGA 80:20 (39 kDa), and a slower release from MP made from PLGA 75:25 (80 kDa) and PLGA 85:15 (62 kDa). It has been demonstrated that Mw plays an essential role in the degradation rate of PLGA. In our study, the PLGA 80:20 has the lowest Mw (39 kDa) and this is most likely why this formulation released adenosine more quickly. Generally, a higher Mw is associated with a slower degradation, while PLGA with a low Mw requires less time for matrix degradation [27,29,30]. The low Mw of PLGA degraded into small fragments which are soluble in an aqueous release medium, thus leading to faster erosion of the microparticles. During erosion, the microparticle matrix becomes increasingly hydrophilic, allowing more water to defuse, thereby improving polymer degradation and thus, adenosine release in a faster and more sustained profile. The slower release of PLGA 85:15 (62 kDa) compared to PLGA 75:25 (80 kDa) can be attributed to a higher ratio of LA in PLGA 85:15 which increases the hydrophobicity and crystallinity of polymer [30] and as a result, reduces the degradability of the polymer in the aqueous release medium.

Furthermore, the data related to the daily release of adenosine illustrated that the PLGA 80:20 provides a sustained total adenosine release of 7.5 μg/ml to 30 μg/ml every two days in the first two weeks (Fig. S6B). Ghribi et al.[15] supplemented osteoinductive media with adenosine with two concentrations of 10^{-4} M (equivalent to ~ 26.7 μg/ml) and 10^{-5} M (equivalent to ~ 2.67 μg/ml) to stimulate osteoblast differentiation of rat bone marrow MSCs, and they showed that the concentration of 10^{-4} M (26.7 μg/ml) can significantly enhance osteoblast differentiation and mineralization *in vitro*. In addition, Kang et al.[18] were able to differentiate human pluripotent stem cells (hPSCs) into osteoblasts by the supplementation of 30 μg/ml of adenosine in growth media. We demonstrate here that supplementation of osteoinductive media with 30 μg/ml of adenosine enhances osteoinduction of hMSCs through the increase of expression of osteocalcin and increased levels of mineralization. In our study, the amount of adenosine delivered from MP made from PLGA 80:20 would be in the range required to achieve osteogenic differentiation *in vitro* based on our data and that from previous studies [15,18]; therefore, this MP formulation (PLGA 80:20) was selected for further biological assessment.

The culture of hMSCs on the selected PLGA/Ad MP in OM media illustrated a statistically significant increase in mineralization compared to cells culture on blank PLGA MP containing no adenosine after 3 weeks of culture. Our data demonstrated that the sustained release of adenosine in 2.5D MP-based scaffolds can induce mineralization by more than 400 %, while supplementation of media in 2D culture with adenosine (30 μg/ml supplemented in the media) can only increase mineralization levels by 64 % approximately. This might be due to the increase in bioavailability of adenosine to the cells when they release from MP (due to the close proximity of the adenosine to the cells upon release) in comparison to when adenosine is supplemented in the media throughout the study. We hypothesized that cells adhered to the surface of PLGA/Ad MP when they were cultured on the scaffolds, localization of released adenosine adjacent to the cell membrane can be more efficient in triggering cell signalling pathways.

The genetic and metabolic responses of hMSCs cultured on MP/Ad and MP in GM and OM were compared to discover the impact of adenosine on cell signalling pathways and the mechanisms by which adenosine can impact osteogenesis. The release of adenosine in OM altered the gene expression of hMSCs in which the osteogenic gene markers such as BGLAP(osteocalcin) [31] and PHEX [31] were significantly upregulated, and the adipogenic gene marker such as CD36 [32,33] and chon-

drogenic gene markers such as COMP [34] were significantly downregulated. The Reactome pathway analysis from MP/Ad and MP samples demonstrated that the pathways including signalling by GPCR, Beta-catenin independent WNT signalling, and Ca^{2+} pathway signalling were significantly upregulated in MP/Ad samples. It has been demonstrated that adenosine can bind and activate the adenosine A_{2B} receptors (as a member of GPCR) to initiate downstream signalling events that lead to osteogenesis in MSCs [11–15]. Our data corroborates these findings and demonstrates the activation of GPCR and downstream pathways in human MSC populations. The data also showed that ß-catenin independent WNT signalling was upregulated resulting from upregulation of the Ca^{2+} pathway in cells cultured on PLGA/Ad. Adenosine binding to A_{2B}ARs activates the receptors leading to acute G protein-mediated responses including stimulation of the $G_{q/11}$ pathway [9,35,36]. Several studies have demonstrated that Ca^{2+} levels and homeostasis in cells can be controlled by activating $G_{q/11}$ pathways [36–38]. It has been illustrated that G_q activates the phospholipase C (PLC) pathway that can trigger an increase in intracellular calcium levels through calcium release from the endoplasmic reticulum and activation of store-operated calcium channels in the cell membrane [37,39]. The impacts of calcium on cellular functions are mainly mediated by the Ca^{2+}-binding protein that activates the phosphatase calcineurin [9,40], which is able to dephosphorylate target genes to be activated [41]. Upregulation of calcium pathways can stimulate the activation of NFAT, Oct/OAP, NF-κB, ERK1/2, and AP-1 [9,36,37]. In unstimulated cells, the nuclear factor of activated T cells (NFAT) proteins are localized to the cytoplasm by hyperphosphorylation of the N-terminal regulatory domain. Signalling pathways that promote a sustained influx of calcium activate the phosphatase, calcineurin, which dephosphorylates the regulatory domain and exposes a nuclear localization sequence [40,42]. In the nucleus, NFAT proteins cooperate with other transcription factors, such as AP-1 and osterix, to regulate the transcription of various genes [43,44]. including ALP, Osteocalcin, and collagens [42,44–46]. therefore, delivery of adenosine to hMSCs can enhance osteogenesis and mineralization in OM/GM by upregulation of Ca^{2+} pathways through the A_{2B}AR-G-PLC pathway. There are some differences in the impact of released adenosine on cell signalling pathways between samples in OM and GM. First, the presence of osteoinductive factors (DEX, AAP, BGP) demonstrates a strong synergistic effect with adenosine, resulting in a significant upregulation of the A_{2B}AR-G-PLC-Ca^{2+}-NFAT signalling pathway. In contrast, the upregulation of this pathway in cells cultured in GM is not statistically significant; in fact, the presence of DEX, AAP, and BGP facilitate induction of cells through the A_{2B}AR-G-PLC-Ca^{2+}-NFAT signalling pathway. Furthermore, the hedgehog ligand biogenesis and Wnt ligand biogenesis pathways were upregulated in OM and downregulated in GM; conversely, the glucagon type ligand-receptor pathway was downregulated in OM and upregulated in GM. Hedgehog signalling [47,48] and Wnt signalling [49,50] can influence bone metabolism and bone repair and can interact with the Ca^{2+}-NFAT signalling pathway. It has been demonstrated that the glucagon-type receptor pathway plays an important role in adipogenesis and lipid metabolism [51,52]. When the glucagon receptor is activated, Gαs can induce the adenylate cyclase (AC) pathway to activate the cyclic adenosine monophosphate (cAMP) [9]. cAMP can activate the cyclic AMP response element binding protein (CREB) which has been shown to be necessary and sufficient for adipogenesis [53,54]. Also, activation of Gαi results in the inhibition of the cAMP pathway [9]. Our data analysis suggested that the factors in OM (DEX, AAP, and BGP) enrich the A_{2B}AR-G-PLC–Ca^{2+}-NFAT signalling pathway and enhance osteogenesis through the upregulation of hedgehog/Wnt ligand biogenesis pathways and inhibition of adipogenesis through the downregulation of glucagon type ligand-receptor-cAMP-CREB pathway. Furthermore, the gene expression data analysis also demonstrated that there is a significant upregulation in the extracellular matrix organization pathway when the adenosine is delivered to hMSCs in GM, and this impact was accentuated in OM. Together, the data propose transduction signalling pathways which are depicted in Fig. 6.

Untargeted metabolomics and pathway analysis showed that specific pathways were significantly altered in response to adenosine release, particularly purine metabolism and the pentose phosphate pathway. These findings align with emerging research emphasizing the pivotal role of purines in bone remodelling [55,56]. Adenosine, a key player in purinergic signalling, substantially bolstered purine metabolism pathways due to its inherent involvement in this process [56]. Numerous studies have substantiated adenosine's ability to enhance osteoblast differentiation, primarily mediated through interactions with the A_{2B}AR receptor [15,57–59]. In addition, nucleotides, which are vital local factors in hMSC osteogenic differentiation, are predominantly released via exocytosis from osteoblast cells [60,61]. The release and total amount of ATP, a nucleotide, are notably influenced by the cell's differentiation stage, with mature bone-forming cells capable of up to seven-fold higher ATP release compared to immature cells [60]. This regulation of extracellular nucleotide concentrations involves various factors, including nucleotide-releasing pathways, ectonucleotidases, and the activity of receptor subtypes [62].

Active differentiation of hMSCs is characterized by a marked upregulation of vital pathways such as energy-based pathways, amino acid metabolisms, and aminoacyl tRNA biosynthesis [63–65]. Crucially, our findings indicate that adenosine delivery significantly enriched these pathways, underscoring its importance in facilitating osteogenesis. Glucose, acts as the primary cellular energy source, can participate in the pentose phosphate pathway to synthesize nucleotides or enter the glycolysis pathway, ultimately yielding pyruvate. The produced pyruvate can then enter the TCA cycle within mitochondria, a pivotal step in energy production [66]. Our findings suggest that delivered adenosine augments energy-based pathways and amino acid metabolisms, both of which are essential for osteogenesis. Moreover, recent research has emphasized the critical role of glutamine metabolism in bone physiology [67–71]. Previous research has indicated the active absorption and processing of glutamine in calvaria and long bone explants [67]. Recent studies have underscored the significance of glutamine in the mineralization of matrices within calvarial osteoblast cells [68]. Notably, declines in glutamine utilization by precursor osteoblast cells with aging may play a role in hindering osteoblast differentiation. [69]. Furthermore, glutamine can be oxidatively converted to citrate within the TCA cycle, thus participating in energy production in osteoblast precursors [70]. Additionally, glutamine's role in glutathione production assumes importance, particularly for the survival of implanted osteoblast precursor cells in an *in vivo* murine bone repair model [71]. Collectively, these findings emphasize the substantial contribution of glutamine to osteoinduction and the mineralization of bone cells, as supported by our data showing significant enrichment of the D-Glutamine and D-glutamate metabolism pathway through the release of adenosine from scaffolds in the media.

The comparison between PLGA MP/Ad samples in GM and OM media proved the synergistic effect of adenosine and OM factors, particularly in augmenting aerobic glycolysis and the pentose phosphate pathway, collectively contributing to enhanced osteogenesis. This synergy may be explained by the ability of extracellular PO_4^{3-} (provided by BGP and AAP) to enter cells and mitochondria, serving as a substrate for ATP synthesis [16]. ATP, in turn, is secreted and metabolized into adenosine, promoting osteogenic differentiation of hMSCs through the A_{2B}AR via autocrine and/or paracrine signalling [16]. Additionally, DEX enhances gluconeogenesis and indirectly interacts with energy-based pathways [72,73]. By increasing ATP production, the AMP/ATP ratio is reduced, downregulating AMP-cAMP-CREB signalling and subsequently inhibiting adipogenesis [52–54]. Our comprehensive metabolic analysis reveals that adenosine delivery profoundly impacts metabolic pathways critical for osteogenic differentiation. The enrichment of purine metabolism, energy-based pathways, and glutamine metabolism underscores adenosine's pivotal role in promoting osteogenesis. Moreover, the synergy between adenosine and OM factors, particularly in augmenting aerobic glycolysis and the pentose phosphate pathway, further enhances

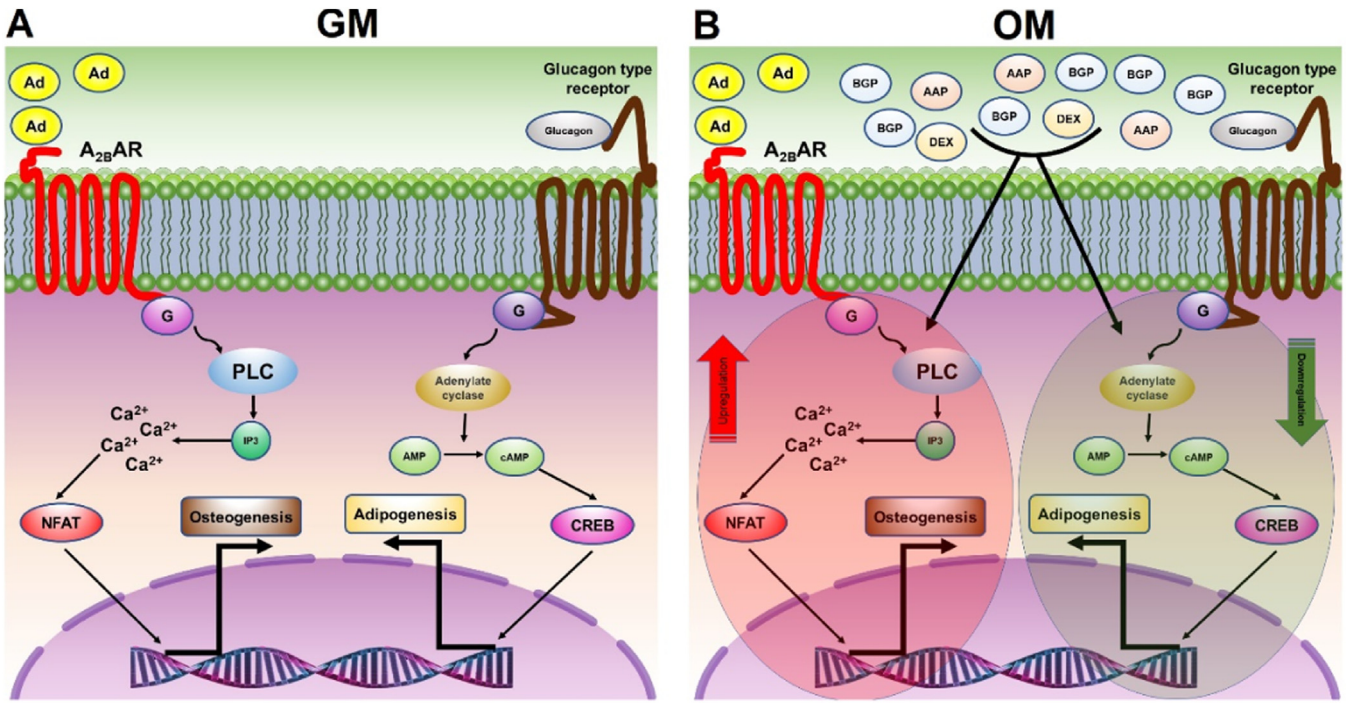

Fig. 6. Schematic model of transduction signalling pathways of hMSCs in the presence of adenosine (Ad) released from microparticles (MP) in (A) growth media (GM) and (B) osteoinductive media (OM).

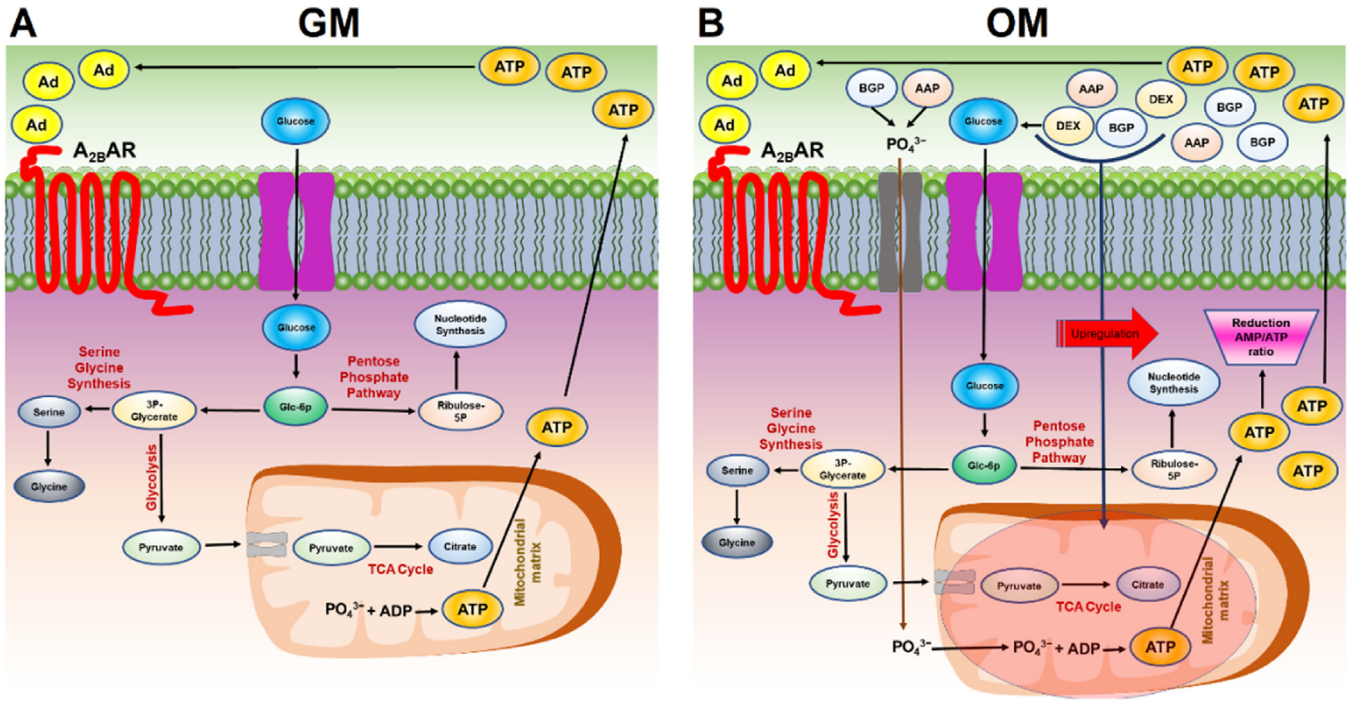

Fig. 7. Schematic model of metabolic pathways of hMSCs in the presence of adenosine (Ad) released from microparticles (MP) in (A) growth media (GM) and (B) osteoinductive media (OM).

osteogenesis. These findings provide valuable insights into the molecular mechanisms that drive osteogenesis, as depicted in Fig. 7.

5. Conclusion

In conclusion, we were able to successfully produce a polymeric microparticle-based delivery system to release adenosine in a sustained manner and demonstrate the synergistic effect, with osteogenic supplements in the media (DEX, BGP, AAP), of the released adenosine on the mineralization and osteogenesis of primary hMSCs. Furthermore, this study demonstrates the role of adenosine on osteogenic differentiation of stromal cells, and mineralization in addition to the role of A_{2B}AR-G-PLC- Ca^{2+}-NFAT signalling and Glycogen-Pyruvate-Citrate pathways in this process. These findings pave the way for new biomaterial strategies in treating critical bone defects and bone metabolic disorders.

Declaration of competing interest

The authors declare that they have no known competing financial interests or personal relationships that could have influenced the work reported in this paper.

CRediT authorship contribution statement

Hadi Hajiali: Conceptualization, Data curation, Formal analysis, Investigation, Methodology, Project administration, Resources, Software, Supervision, Validation, Visualization, Writing – original draft, Writing – review & editing. **Jane McLaren:** Investigation, Writing – review & editing. **Cristina Gonzalez-García:** Investigation. **Salah Abdelrazig:** Data curation, Formal analysis, Investigation, Methodology, Visualization, Writing – review & editing. **Dong-Hyun Kim:** Supervision, Writing – review & editing. **Matthew J. Dalby:** Funding acquisition, Resources, Supervision, Methodology, Writing – review & editing. **Manuel Salmerón-Sánchez:** Funding acquisition, Methodology, Resources, Supervision, Writing – review & editing. **Felicity R.A.J. Rose:** Conceptualization, Funding acquisition, Project administration, Resources, Methodology, Software, Supervision, Writing – review & editing.

Acknowledgments

Financial support was received from Engineering and Physical Sciences Research Council (EPSRC); Reference: EP/P001114/; Engineering growth factor microenvironments - a new therapeutic paradigm for regenerative medicine.

Supplementary materials

Supplementary material associated with this article can be found, in the online version, at doi:10.1016/j.engreg.2024.04.002.

References

[1] R.A. Gosselin, D.J. Conway, J.J. Phillips, R.R. Coughlin, Diseases of the musculoskeletal system, in: Hunter's Tropical Medicine and Emerging Infectious Diseases, Elsevier, 2020, pp. 114–119.
[2] E. Hernlund, et al., Osteoporosis in the European Union: medical management, epidemiology and economic burden: a report prepared in collaboration with the International Osteoporosis Foundation (IOF) and the European Federation of Pharmaceutical Industry Associations (EFPIA), Arch. Osteoporos. 8 (2013) 1–115.
[3] H. Hajiali, L. Ouyang, V. Llopis-Hernandez, O. Dobre, F.R.A.J. Rose, Review of emerging nanotechnology in bone regeneration: progress, challenges, and perspectives, Nanoscale 13 (2021) 10266–10280.
[4] A. Boussahel, C. Rahman, F. Rose, K.M Shakesheff, An injectable scaffold with sustained release of rhBMP2 for bone regeneration, J. Pharm. Pharmacol. 62 (2010) 1499–1500 WILEY-BLACKWELL COMMERCE PLACE, 350 MAIN ST, MALDEN 02148, MA USA.
[5] O. Qutachi, et al., Improved delivery of PLGA microparticles and microparticle–cell scaffolds in clinical needle gauges using modified viscosity formulations, Int. J. Pharm. 546 (2018) 272–278.
[6] G.T.S. Kirby, et al., PLGA-based microparticles for the sustained release of BMP-2, Polymers (Basel) 3 (2011) 571–586.
[7] A.J. Kimple, D.E. Bosch, P.M. Giguère, D.P. Siderovski, Regulators of G-protein signaling and their Gα substrates: promises and challenges in their use as drug discovery targets, Pharmacol. Rev. 63 (2011) 728–749.
[8] D. Keinan, et al., Role of regulator of G protein signaling proteins in bone, Front. Biosci. (Landmark Ed. 19 (2014) 634.
[9] J. Jules, S. Yang, W. Chen, Y.-P. Li, Role of regulators of G protein signaling proteins in bone physiology and pathophysiology, Prog. Mol. Biol. Transl. Sci. 133 (2015) 47–75.
[10] C.R. McCudden, M.D. Hains, R.J. Kimple, D.P. Siderovski, F.S. Willard, G-protein signaling: back to the future, Cell. Mol. Life Sci. 62 (2005) 551–577.
[11] M.L. Trincavelli, et al., Osteoblast differentiation and survival: a role for A2B adenosine receptor allosteric modulators, Biochim. Biophys. Acta (BBA)-Molecular Cell Res. 1843 (2014) 2957–2966.
[12] C. Corciulo, T. Wilder, B.N. Cronstein, Adenosine A2B receptors play an important role in bone homeostasis, Purinergic Signal 12 (2016) 537–547.
[13] H.-B. Ruan, J.P. Singh, M.-D. Li, J. Wu, X. Yang, Cracking the O-GlcNAc code in metabolism, Trends Endocrinol. Metab. 24 (2013) 301–309.
[14] K. Nishimura, et al., Development of defective and persistent Sendai virus vector: a unique gene delivery/expression system ideal for cell reprogramming, J. Biol. Chem. 286 (2011) 4760–4771.
[15] B. Gharibi, A.A. Abraham, J. Ham, B.A.J. Evans, Adenosine receptor subtype expression and activation influence the differentiation of mesenchymal stem cells to osteoblasts and adipocytes, J. Bone Miner. Res. 26 (2011) 2112–2124.
[16] Y.-R.V. Shih, et al., Calcium phosphate-bearing matrices induce osteogenic differentiation of stem cells through adenosine signaling, Proc. Natl. Acad. Sci 111 (2014) 990–995.
[17] H. Kang, Y.-R.V. Shih, S. Varghese, Biomineralized matrices dominate soluble cues to direct osteogenic differentiation of human mesenchymal stem cells through adenosine signaling, Biomacromolecules 16 (2015) 1050–1061.
[18] H. Kang, Y.-R.V. Shih, M. Nakasaki, H. Kabra, S. Varghese, Small molecule–driven direct conversion of human pluripotent stem cells into functional osteoblasts, Sci. Adv. 2 (2016) e1600691.
[19] L.J. White, et al., Accelerating protein release from microparticles for regenerative medicine applications, Mater. Sci. Eng. C 33 (2013) 2578–2583.
[20] R.W. Sands, D.J. Mooney, Polymers to direct cell fate by controlling the microenvironment, Curr. Opin. Biotechnol. 18 (2007) 448–453.
[21] J.C. Middleton, A.J. Tipton, Synthetic biodegradable polymers as orthopedic devices, Biomaterials 21 (2000) 2335–2346.
[22] R. Arce, L. Marínez, E. Danielsen, The photochemistry of adenosine: intermediates contributing to its photodegradation mechanism in aqueous solution at 298 K and characterization of the major product, Photochem. Photobiol. 58 (1993) 318–328.
[23] S. Halfon, N. Abramov, B. Grinblat, I. Ginis, Markers distinguishing mesenchymal stem cells from fibroblasts are downregulated with passaging, Stem Cells Dev. 20 (2011) 53–66.
[24] A. Surrati, S. Evseev, F. Jourdan, D.-H. Kim, V. Sottile, Osteogenic response of human mesenchymal stem cells analysed using combined intracellular and extracellular metabolomic monitoring, Cell. Physiol. Biochem. 55 (2021).
[25] Z. Pang, et al., Using MetaboAnalyst 5.0 for LC–HRMS spectra processing, multi-omics integration and covariate adjustment of global metabolomics data, Nat. Protoc. 17 (2022) 1735–1761.
[26] O. Fiehn, Combining genomics, metabolome analysis, and biochemical modelling to understand metabolic networks, Comp. Funct. Genomics 2 (2001) 155–168.
[27] S. Ravi, et al., Development and characterization of polymeric microspheres for controlled release protein loaded drug delivery system, Indian J. Pharm. Sci. 70 (2008) 303.
[28] D. Essa, P.P.D. Kondiah, Y.E. Choonara, V. Pillay, The design of poly (lactide-co-glycolide) nanocarriers for medical applications, Front. Bioeng. Biotechnol. 8 (2020) 48.
[29] Y. Su, et al., PLGA-based biodegradable microspheres in drug delivery: recent advances in research and application, Drug Deliv. 28 (2021) 1397–1418.
[30] E. Lagreca, et al., Recent advances in the formulation of PLGA microparticles for controlled drug delivery, Prog. Biomater. 9 (2020) 153–174.
[31] W. Huang, S. Yang, J. Shao, Y.-P. Li, Signaling and transcriptional regulation in osteoblast commitment and differentiation, Front. Biosci. J. Virtual Libr. 12 (2007) 3068.
[32] V. Christiaens, M. Van Hul, H.R. Lijnen, I. Scroyen, CD36 promotes adipocyte differentiation and adipogenesis, Biochim. Biophys. Acta (BBA)-General Subj. 1820 (2012) 949–956.
[33] H. Gao, et al., CD36 is a marker of human adipocyte progenitors with pronounced adipogenic and triglyceride accumulation potential, Stem Cells 35 (2017) 1799–1814.
[34] C. Acharya, et al., Cartilage oligomeric matrix protein and its binding partners in the cartilage extracellular matrix: interaction, regulation and role in chondrogenesis, Matrix Biol. 37 (2014) 102–111.
[35] Y. Sun, P. Huang, Adenosine A2B receptor: from cell biology to human diseases, Front. Chem. 4 (2016) 37 2016.
[36] Z. Gao, T. Chen, M.J. Weber, J. Linden, A2B adenosine and P2Y2 receptors stimulate mitogen-activated protein kinase in human embryonic kidney-293 cells: cross-talk between cyclic AMP and protein kinase C pathways, J. Biol. Chem. 274 (1999) 5972–5980.
[37] M. Zayzafoon, Calcium/calmodulin signaling controls osteoblast growth and differentiation, J. Cell. Biochem. 97 (2006) 56–70.
[38] M. Panjehpour, M. Castro, K. Klotz, Human breast cancer cell line MDA-MB-231 expresses endogenous A2B adenosine receptors mediating a Ca2+ signal, Br. J. Pharmacol. 145 (2005) 211–218.
[39] E.M. Brown, R.J. MacLeod, Extracellular calcium sensing and extracellular calcium signaling, Physiol. Rev. 81 (2001) 239–297.
[40] P.G. Hogan, L. Chen, J. Nardone, A. Rao, Transcriptional regulation by calcium, calcineurin, and NFAT, Genes Dev. 17 (2003) 2205–2232.
[41] E.M. Brown, et al., Cloning and characterization of an extracellular Ca2+-sensing receptor from bovine parathyroid, Nature 366 (1993) 575–580.
[42] D. Sitara, A.O. Aliprantis, Transcriptional regulation of bone and joint remodeling by NFAT, Immunol. Rev. 233 (2010) 286–300.
[43] S.-H. Im, A. Rao, Activation and deactivation of gene expression by Ca 2+/Calcineurin-NFAT-mediated signaling, Mol. Cells (Springer Sci. Bus. Media BV) 18 (2004).
[44] T. Koga, et al., NFAT and Osterix cooperatively regulate bone formation, Nat. Med. 11 (2005) 880–885.
[45] M.-K. Choo, H. Yeo, M. Zayzafoon, NFATc1 mediates HDAC-dependent transcriptional repression of osteocalcin expression during osteoblast differentiation, Bone 45 (2009) 579–589.
[46] H. Yeo, L.H. Beck, J.M. McDonald, M. Zayzafoon, Cyclosporin A elicits dose-dependent biphasic effects on osteoblast differentiation and bone formation, Bone 40 (2007) 1502–1516.
[47] J. Yang, P. Andre, L. Ye, Y.-Z. Yang, The Hedgehog signalling pathway in bone formation, Int. J. Oral Sci. 7 (2015) 73–79.

[48] W.-T. Lv, et al., Regulation of hedgehog signaling offers a novel perspective for bone homeostasis disorder treatment, Int. J. Mol. Sci. 20 (2019) 3981.
[49] J.H. Kim, et al., Wnt signaling in bone formation and its therapeutic potential for bone diseases, Ther. Adv. Musculoskelet. Dis. 5 (2013) 13–31.
[50] K.S. Houschyar, et al., Wnt pathway in bone repair and regeneration–what do we know so far, Front. Cell Dev. Biol. 6 (2019) 170.
[51] T.D. Challa, et al., Regulation of adipocyte formation by GLP-1/GLP-1R signaling, J. Biol. Chem. 287 (2012) 6421–6430.
[52] K.D. Galsgaard, J. Pedersen, F.K. Knop, J.J. Holst, N.J. Wewer Albrechtsen, Glucagon receptor signaling and lipid metabolism, Front. Physiol. 10 (2019) 413.
[53] E.D. Rosen, C.J. Walkey, P. Puigserver, B.M. Spiegelman, Transcriptional regulation of adipogenesis, Genes Dev. 14 (2000) 1293–1307.
[54] J.E.B. Reusch, L.A. Colton, D.J. Klemm, CREB activation induces adipogenesis in 3T3-L1 cells, Mol. Cell. Biol. 20 (2000) 1008–1020.
[55] A. Hoebertz, T.R. Arnett, G. Burnstock, Regulation of bone resorption and formation by purines and pyrimidines, Trends Pharmacol. Sci. 24 (2003) 290–297.
[56] M. Carluccio, et al., Adult mesenchymal stem cells: is there a role for purine receptors in their osteogenic differentiation? Purinergic Signal 16 (2020) 263–287.
[57] M.A. Costa, et al., On the role of subtype selective adenosine receptor agonists during proliferation and osteogenic differentiation of human primary bone marrow stromal cells, J. Cell. Physiol. 226 (2011) 1353–1366.
[58] W. He, A. Mazumder, T. Wilder, B.N. Cronstein, Adenosine regulates bone metabolism via A1, A2A, and A2B receptors in bone marrow cells from normal humans and patients with multiple myeloma, FASEB J. 27 (2013) 3446–3454.
[59] S.H. Carroll, et al., A2B adenosine receptor promotes mesenchymal stem cell differentiation to osteoblasts and bone formation *in vivo*, J. Biol. Chem. 287 (2012) 15718–15727.
[60] I.R. Orriss, et al., Hypoxia stimulates vesicular ATP release from rat osteoblasts, J. Cell. Physiol. 220 (2009) 155–162.
[61] M. Romanello, et al., Autocrine/paracrine stimulation of purinergic receptors in osteoblasts: contribution of vesicular ATP release, Biochem. Biophys. Res. Commun. 331 (2005) 1429–1438.
[62] J.B. Noronha-Matos, et al., Role of ecto-NTPDases on UDP-sensitive P2Y6 receptor activation during osteogenic differentiation of primary bone marrow stromal cells from postmenopausal women, J. Cell. Physiol. 227 (2012) 2694–2709.
[63] W.-C. Lee, A.R. Guntur, F. Long, C.J. Rosen, Energy metabolism of the osteoblast: implications for osteoporosis, Endocr. Rev. 38 (2017) 255–266.
[64] P.M. Tsimbouri, et al., Using nanotopography and metabolomics to identify biochemical effectors of multipotency, ACS Nano 6 (2012) 10239–10249.
[65] M. Tencerova, et al., Metabolic programming determines the lineage-differentiation fate of murine bone marrow stromal progenitor cells, Bone Res. 7 (2019) 1–14.
[66] J.I. Messer, M.R. Jackman, W.T. Willis, Pyruvate and citric acid cycle carbon requirements in isolated skeletal muscle mitochondria, Am. J. Physiol. Physiol. 286 (2004) C565–C572.
[67] R.M. Biltz, J.M. Letteri, E.D. Pellegrino, A. Palekar, L.M. Pinkus, Glutamine metabolism in bone, Miner. Electrolyte Metab 9 (1983) 125–131.
[68] P.M. Brown, J.D. Hutchison, J.C. Crockett, Absence of glutamine supplementation prevents differentiation of murine calvarial osteoblasts to a mineralizing phenotype, Calcif. Tissue Int. 89 (2011) 472–482.
[69] T. Huang, et al., Aging reduces an ERRalpha-directed mitochondrial glutaminase expression suppressing glutamine anaplerosis and osteogenic differentiation of mesenchymal stem cells, Stem Cells 35 (2017) 411–424.
[70] C.M. Karner, E. Esen, A.L. Okunade, B.W. Patterson, F. Long, Increased glutamine catabolism mediates bone anabolism in response to WNT signaling, J. Clin. Invest. 125 (2015) 551–562.
[71] S. Stegen, et al., HIF-1α promotes glutamine-mediated redox homeostasis and glycogen-dependent bioenergetics to support postimplantation bone cell survival, Cell Metab. 23 (2016) 265–279.
[72] G. Mazziotti, C. Gazzaruso, A. Giustina, Diabetes in cushing syndrome: basic and clinical aspects, Trends Endocrinol. Metab. 22 (2011) 499–506.
[73] A. Rafacho, H. Ortsä ter, A. Nadal, I. Quesada, Glucocorticoid treatment and endocrine pancreas function: implications for glucose homeostasis, insulin resistance and diabetes, J. Endocrinol. 223 (2014) R49–R62.